

## Steady-State Confinement of Non-neutral Plasmas by Rotating Electric Fields

X.-P. Huang,\* F. Anderegg, E. M. Hollmann, C. F. Driscoll, and T. M. O'Neil

*Physics Department and Institute for Pure and Applied Physical Sciences, University of California at San Diego,  
La Jolla, California 92093-0319*

(Received 25 October 1996)

We apply “rotating wall” electric fields to spin up a non-neutral plasma in a Penning-Malmberg trap, resulting in steady-state confinement (weeks) of up to  $10^9$   $\text{Mg}^+$  ions. The resulting ion columns can be near global thermal equilibrium, with near-uniform temperature and rotation frequency. The equilibrated plasma  $\mathbf{E} \times \mathbf{B}$  rotation rate  $f_E$  is observed to be somewhat less than the drive frequency  $f_w$ , with slip  $\Delta f \equiv f_w - f_E$  depending on temperature as  $\Delta f \propto T^{1/2}$  for  $0.05 \leq T \leq 5$  eV. Dynamic measurements of applied torque versus slip frequency show plasma spin up and compression for  $\Delta f > 0$  and plasma slowing and expansion for  $\Delta f < 0$ . By gradually increasing  $f_w$ , density compression up to 20% of the Brillouin density limit has been achieved. Heating resonances and hysteresis in plasma parameters are also observed. [S0031-9007(97)02311-9]

PACS numbers: 52.25.Wz, 32.80.Pj, 52.55.Dy

Unneutralized plasmas are confined in Penning traps [1] for a variety of experiments and technologies in plasma physics [2], precision spectroscopy [3], Coulomb crystals [4], and antimatter research [5,6]. Conservation of (canonical) angular momentum  $P_\theta$  in a cylindrically symmetric trap suggests that the plasma should be confined forever [7]. In practice, small static field errors and background neutral gas [8] exert a drag on the rotating plasma, causing slow plasma expansion and eventual particle loss [9–11]. Two techniques are commonly used to counter this expansion: torques from laser beams give steady-state confinement of  $10^3$ – $10^6$  ions when resonant optical transitions are available [12], and “sideband cooling” from rf fields at the sum of the axial bounce and magnetron frequencies compresses small numbers of particles trapped with quadratic harmonic potentials [13,14].

Here, we show that a “rotating wall” electric field asymmetry [15,16] can balance or exceed the drag on a plasma of up to  $10^9$   $\text{Mg}^+$  ions in a cylindrical Penning-Malmberg trap, resulting in steady-state confinement for weeks, or in density compression up to 20% of the Brillouin limit. Laser-induced-fluorescence (LIF) diagnostics show that the ion plasma can have near-uniform density, temperature, and rotation frequency, i.e., that it is near global thermal equilibrium. The equilibrium plasma  $\mathbf{E} \times \mathbf{B}$  rotation frequency at  $r = 0$ ,  $f_E(0)$ , is somewhat less than the applied drive frequency  $f_w$ , with slip  $\Delta f \equiv f_w - f_E(0)$  proportional to the thermal ion axial bounce frequency  $f_b$  over several decades in temperature.

Dynamic measurements give the applied torque  $\tau \propto dP_\theta/dt$  versus  $\Delta f$ , showing that the rotating field causes plasma compression and spin up when the drive rotates faster than the plasma ( $\Delta f > 0$ ), and causes plasma expansion when  $\Delta f < 0$ . Just as static perturbations produce a drag that slows the plasma rotation, the field rotating faster than the plasma tends to increase the plasma rotation; this experimentally observed and intuitively reasonable effect can be understood as a consequence of the second law of

thermodynamics [17]. This process is analogous to an induction motor, since the applied electric field both creates and couples to a perturbation in the rotating plasma. The rotating wall technique may also be related to attempts to spin up or stabilize neutral plasmas by coupling to resonant layers [18]. The drive necessarily results in some plasma heating, and additional heating can arise when unwanted spatial or temporal components of the applied field resonantly excite plasma modes. Since the plasma/field coupling is temperature dependent, these effects can result in hysteresis or loss of plasma equilibrium.

Figure 1 shows the ion trap with LIF diagnostics, and a schematic representation of the rotating field drive. The ions from a metal vacuum arc [19] are trapped within conducting cylinders of radius  $R_w = 2.86$  cm. A uniform axial field  $\mathbf{B} = 4$  T ( $-\hat{z}$ ) provides radial confinement, and trap voltages (200 V) on end cylinders give axial confinement of an ion column of length  $L_p \approx 10$  cm and radius  $R_p \approx 1$  cm, with no confinement of electrons. The LIF and ion cyclotron mass spectroscopy [20] indicate that the trapped ion plasmas are about 70%  $\text{Mg}^+$ , with the remainder being mainly  $\text{MgH}_n^+$  and  $\text{H}_n^+$ . The ions typically cool to  $T \approx 0.05$  eV due to collisions with neutrals, with collision rate  $\nu_{iN} \approx 0.1$   $\text{sec}^{-1}$  at  $P = 3 \times 10^{-9}$  Torr of  $\text{H}_2$ . With no rotating field drive, the plasma expands radially with characteristic time of about 2000 sec due to ambient field errors and neutral collisions [9,20].

The rotating field drive consists of sinusoidal voltages  $\Phi_{wj}$  applied to eight wall sectors at  $\theta_j = 2\pi j/8$ , with  $\Phi_{wj} = A_w \cos[m(\theta_j - 2\pi f_w t)]$ . Fields with  $m = 1$  and  $m = 2$  are described here; in general,  $m = 1$  is the most effective because the resulting electric field is nonzero at the origin, and because the unwanted co- and counterrotating spatial harmonics are less significant.

The plasma density, temperature, and rotation velocity profiles are obtained from a 0.5 mW cw, 280 nm laser beam which is scanned across the plasma, with a

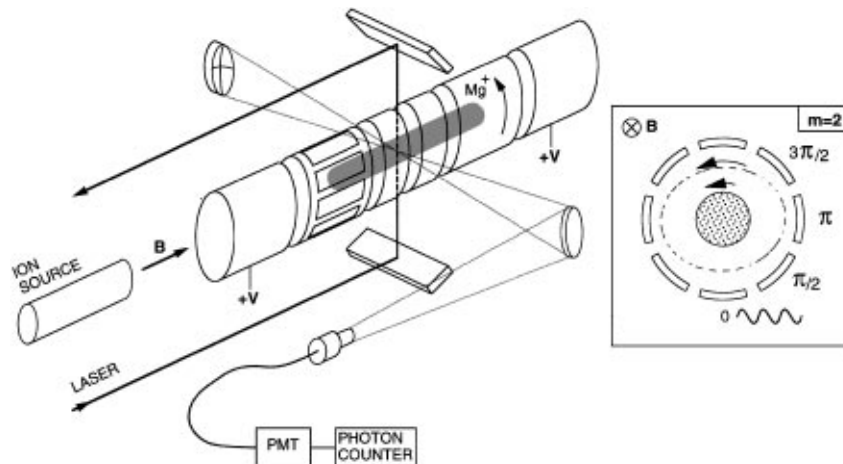


FIG. 1. Ion trap with perpendicular LIF diagnostics, and schematic of  $m = 2$  rotating field wall sector signals.

detection volume of  $1 \text{ mm}^2 \times 3 \text{ mm}$  ( $\Delta x \Delta z \Delta y$ ). At each radial position, the frequency of the laser (bandwidth  $\approx 1 \text{ MHz}$ ) is scanned  $60 \text{ GHz}$  across a  $3^2S_{1/2} \rightarrow 3^2P_{3/2}$  “cyclone” transition of  $\text{Mg}^+$  in  $1.7 \text{ sec}$  to obtain the  $\theta$ -averaged ion velocity distribution, and the density  $n(r)$ , temperature  $T(r)$ , and total rotation velocity  $v_{\text{tot}}(r)$  are obtained by fitting to a shifted Maxwellian distribution. This weak diagnostic beam applies negligible torque on the plasma. The plasma is near-Maxwellian, since perturbations are weak compared to the ion-ion velocity scattering rate  $\nu_{ii} \equiv (16\sqrt{\pi}/15) nb^2\bar{v} \ln(r_c/b) \approx (1.0/\text{sec})T^{-3/2}(n/10^7)$ , where  $\bar{v} \equiv (T/M)^{1/2}$ ,  $b \equiv e^2/T$ ,  $r_c \equiv \bar{v}/(eB/Mc)$ . The LIF detection efficiency is calibrated by the total charge measured when the plasma is dumped, so the measured density  $n(r)$  includes contributions from the impurity ions. For  $T > 10^{-2} \text{ eV}$ , there is negligible centrifugal separation of the ion species present in the trap [21].

Figure 2 shows the profiles of density, temperature, and total rotation velocity for a plasma measured 31 h after being created. This plasma is in dynamical equilibrium, with torques from the rotating  $m = 2$  field bal-

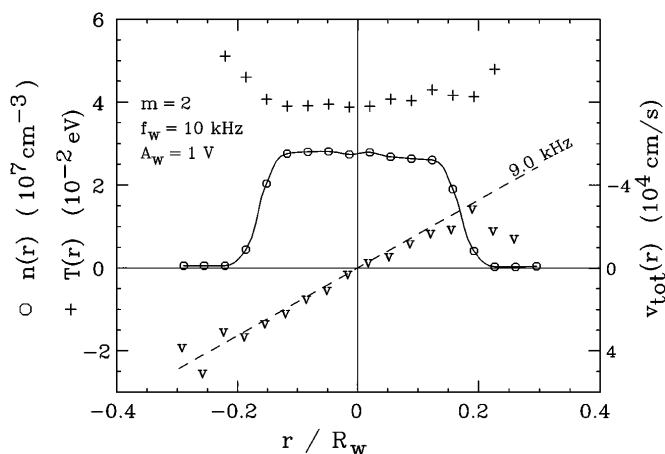


FIG. 2.  $\theta$ -averaged radial profiles of ion density ( $\circ$ ), temperature ( $+$ ), and total fluid rotation velocity ( $\nabla$ ) for a steady-state ion cloud near thermal equilibrium, driven by  $f_w = 10 \text{ kHz}$ .

ancing the drags from static field errors and neutral collisions. The steady-state plasma is characterized by flat density and temperature profiles and rigid rotation in the bulk of the plasma, indicating that it is near global thermal equilibrium. The total rotation rate is given by  $f_{\text{tot}}(r) \equiv v_{\text{tot}}(r)/2\pi r$ , and the dashed line in Fig. 2 shows that the fitted central rotation rate  $f_{\text{tot}}(0) = 9.0 \text{ kHz}$  is significantly less than the drive frequency  $f_w = 10 \text{ kHz}$ . The diamagnetic drift velocity  $v_d(r) \equiv (-c/enB)(\partial/\partial r)(nT)$  is negligible for this cold plasma except at the edge, but  $v_d$  can be large for hot plasmas. We obtain the  $\mathbf{E} \times \mathbf{B}$  drift velocity as  $v_E(r) \equiv v_{\text{tot}} - v_d$ , and the  $\mathbf{E} \times \mathbf{B}$  rotation frequency as  $f_E(r) \equiv v_E/2\pi r$ .

Motivated by single-particle theory, we define the central slip frequency as  $\Delta f \equiv f_w - f_E(0)$ ; the slip relative to the fluid rotation frequency  $f_{\text{tot}}(0)$  could alternately be used, with little change in the conclusions that follow. For fixed  $m$  and  $f_w$ , the slip of a given plasma decreases as the drive voltage  $A_w$  increases from zero, and for  $A_w \gtrsim 0.5 \text{ V}$ , the slip asymptotes to a constant value. This slip at large  $A_w$  does, however, depend on plasma temperature, as  $\Delta f \propto T^{1/2}$ . To characterize the temperature, we define the thermal particle bounce frequency  $f_b \equiv \bar{v}/2L_p = (10 \text{ kHz})T^{1/2}(L_p/10)^{-1}$ .

Figure 3 shows the slip  $\Delta f$  versus bounce frequency  $f_b$  for several plasmas confined by  $m = 1$  or  $m = 2$  rotating fields with  $f_w = 20 \text{ kHz}$ . For a given plasma, the temperature is increased by modulating the axial length of the plasma, or decreased by auxiliary laser cooling parallel to  $B$  [4,12]. As the temperature increases from  $1.5 \times 10^{-3}$  to  $5 \text{ eV}$ , the rotating field coupling apparently becomes less effective: the plasma expands, decreasing the central density from  $12$  to  $0.3 \times 10^7 \text{ cm}^{-3}$ , decreasing  $f_E$ , and therefore increasing the slip until the rotating field torque again balances the background drag. Over this wide range of plasma temperature, we observe  $\Delta f \approx (0.5 - 1)f_b$ , delineated by the two dashed lines. This  $T^{1/2}$  dependence suggests that the field-plasma coupling involves single-particle bounce-rotation resonances

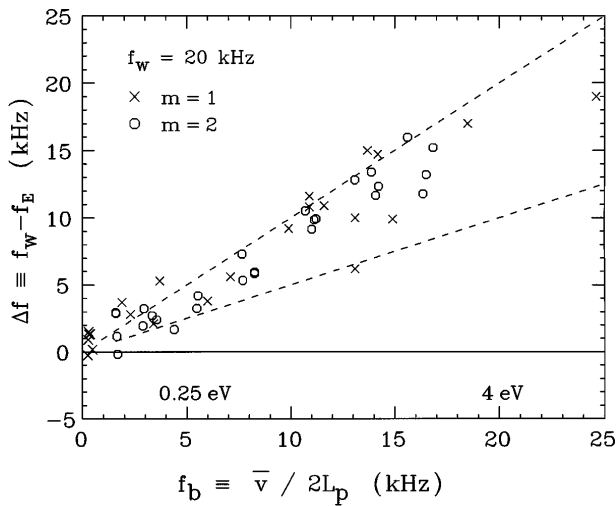


FIG. 3. Measured  $\mathbf{E} \times \mathbf{B}$  slip frequency vs the thermal axial bounce frequency, for  $f_w = 20$  kHz. The dashed lines show  $\Delta f = f_b$  and  $\Delta f = 0.5f_b$ .

[17], but collective effects such as waves propagating at  $\bar{v}$  are not precluded. Experiments have shown, moreover, that applied fields with no  $z$  dependence couple less well to moderate temperature plasmas, supporting a  $z$ -dependent interaction. Note that the collisionality varies widely in this data: taking  $n = 10^7 \text{ cm}^{-3}$ , we obtain  $2.5 \times 10^5 > f_b/\nu_{ii} > 25$  for  $5 > T > 0.05 \text{ eV}$ , whereas ions in the laser-cooled plasmas at  $T \approx 1.5 \text{ meV}$  diffuse rather than bounce axially, with  $f_b/\nu_{ii} \approx 0.02$ .

We have measured the torque applied by the rotating field as a function of the slip applied by the rotating rate of compression or expansion following an abrupt change in  $f_w$ . Figure 4 shows the measured scaled torque  $\tau$  from an  $m = 1$ ,  $f_w = 50$  kHz rotating field versus  $\Delta f/f_b$  for two different plasmas. The torque is proportional to the rate of change of the mean-square radius of the plasma, since the angular momentum

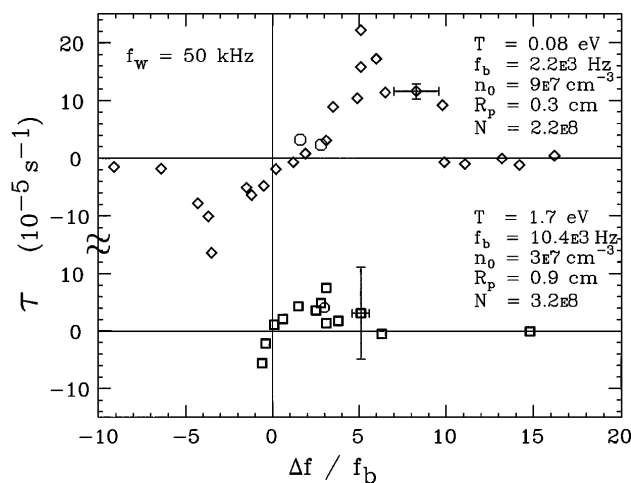


FIG. 4. Measured torque vs slip frequency from an  $m = 1$  rotating field at 50 kHz acting on two plasmas differing mainly by a factor of 20 in temperature.

$P_\theta$  is predominantly electromagnetic rather than kinetic. That is,  $P_\theta \approx (eBL_p/2c) \int 2\pi r dr (R_w^2 - r^2)n \equiv (NeB/2c)(R_w^2 - \langle r^2 \rangle)$ , where  $N$  is the total number of ions. We define the scaled torque as  $\tau \equiv (2c/eBNR_w^2)(d/dt)P_\theta = -(d/dt)\langle r^2 \rangle/R_w^2$ .

In equilibrium, the rotating field torque  $\tau_{\text{eq}} > 0$  exactly balances the background drag and the plasma has a slip  $\Delta f > 0$ ; this equilibrium is represented by circles in Fig. 4. We obtain  $\tau_{\text{eq}}$  by abruptly turning the rotating field off and measuring the expansion rate  $-\tau_{\text{eq}}$ . Alternately, if  $f_w$  (and therefore  $\Delta f$ ) is abruptly changed, the plasma contracts (or expands) at a rate  $\tau_{\delta f_w}$  proportional to the amount the modified torque differs from the background drag. The total torque  $\tau(\Delta f)$  supplied by the slipping field is then  $\tau(\Delta f) = \tau_{\delta f_w} + \tau_{\text{eq}}$ . The torque is positive (giving plasma compression) for  $\Delta f > 0$ , negative for  $\Delta f < 0$ , and goes to zero for large  $|\Delta f|$ . Also, the torque appears to be less for hot plasmas, as noted above. The scatter in the data arises from inaccuracies in measuring  $f_E(0)$  and  $\langle r^2 \rangle$  (shown by representative error bars), and from irreproducibility in reequilibrating to the same plasma after each temporary change of  $f_w$ .

The experimental observations agree qualitatively but not quantitatively with a recent kinetic theory [17] of the radial transport of particles satisfying a bounce/rotation resonance. Theoretical estimates of the torque have the same form as Fig. 4, but are 50–200 times larger than observed experimentally. However, over much of the experimental parameter regime, the assumptions of this theory are not well satisfied; for example, the length of the ion plasma may not respond adiabatically to the applied perturbation. In contrast, experiments on the related effect of diocotron mode damping from “rotational pumping” of the length of electron plasmas show close agreement with the kinetic theory in the adiabatic regime [22].

The rotating field torque allows us to control the plasma density and rotation frequency by gradually varying the frequency of the drive. Figure 5 shows the evolution of the central charge density  $n(0)$  and temperature  $T(0)$  as  $f_w$  is ramped; for generality, ramps with  $m = 1$  and  $m = 2$  are both shown. The dashed line in Fig. 5(a) indicates the “no-slip” condition where  $\Delta f = 0$ , i.e.,  $f_E(0) = f_w$ . The density increases almost linearly with drive frequency, up to about 13% of the Brillouin density limit  $n_B \equiv B^2/8\pi M c^2$ . By adding laser cooling, compression above 20% of the Brillouin limit has been observed. For  $f_w \geq 100$  kHz, the plasma temperature and slip increase markedly; note that here,  $\Delta f \approx (4 - 10)f_b$ , and the plasmas are not near thermal equilibrium, having nonuniform density, temperature, and rotation profiles. Above 150 kHz, the plasma is no longer in equilibrium with the drive: the plasma is expanding and cooling as  $f_w$  is ramped.

Heating resonances associated with  $(m, k)$  plasma modes are clearly visible in the central plasma temperature: these modes vary as  $\cos(k\pi z/L_p) \exp(im\theta)$ . The strongest heating resonances are  $m = 0, k \neq 0$  plasma modes excited by the small unwanted  $m = 0$  component

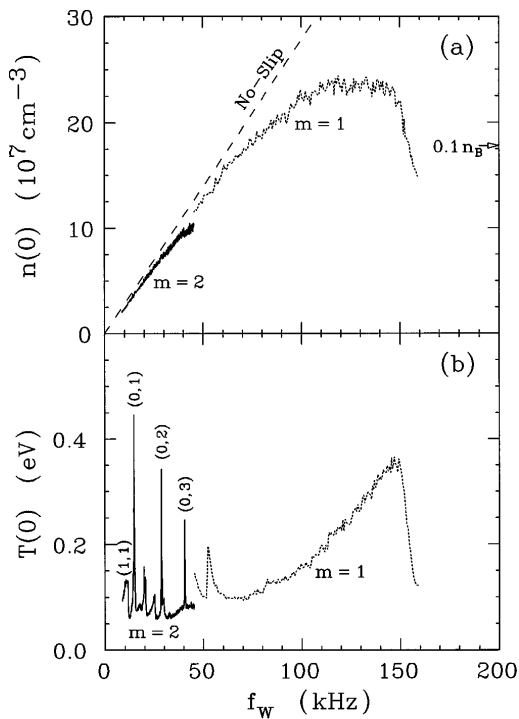


FIG. 5. Evolution of central ion density (a) and temperature (b) during gradual ramp of rotating field frequency. Density compression by an order of magnitude up to 13% Brillouin density limit  $n_B$  is shown in (a), and heating resonances due to excitation of  $k \neq 0$  plasma modes are observed in (b).

of the nominally  $m = 1$  or  $m = 2$  rotating field. By detecting the waves induced with an intentionally enlarged  $m = 0$  drive component, we find unambiguous agreement with Trivelpiece-Gould mode theory [23], including shifts in the resonances as the plasma length is varied. Interestingly, the broad (1, 1) resonance is a mode propagating in the same direction as, but faster than, the plasma rotation. Resonances presumably give stronger couplings to the rotating field, but the resonance is more difficult to maintain experimentally.

We also note that for the data of Fig. 5, the drive frequency  $f_w$  was ramped through the heating resonances before the plasma could fully relax to a stationary density and temperature profile; indeed, resonant heating may cause increased slip, so that the plasma density remains constant as  $f_w$  is increased over a small range. In practice, numerous hysteresis loops with respect to  $f_w$  are observed, due to the density, temperature, and shear dependence of the rotating wall drive and of the background drags.

In summary, an applied rotating field couples torque and energy into a confined ion plasma, providing a steady-state balance against the drag and cooling from field asymmetries and neutrals. Near-thermal-equilibrium plasmas can thus be confined indefinitely, over a wide range of plasma parameters. The coupling is observed for regimes of low and high collisionality, with slip varying approximately as  $T^{1/2}$ . We believe this technique will be applicable to a variety of trapping experiments.

We gratefully acknowledge theoretical contributions by Dr. D.H.E. Dubin and Dr. S.M. Crooks. We thank Dr. D.J. Wineland, Dr. J.J. Bollinger, and Dr. J.C. Bergquist for advice on the experiment. This research is supported by the Office of Naval Research (N00014-89-J-1714) and the National Science Foundation (PHY91-20240).

\*Current address: Time and Frequency Division, National Institute of Standards and Technology, Boulder, CO 80303.

- [1] F.M. Penning, *Physica* (Utrecht) **3**, 873 (1936); H.G. Dehmelt, *Adv. At. Mol. Phys.* **3**, 53 (1967); **5**, 109 (1969); J.H. Malmberg and J.S. deGrassie, *Phys. Rev. Lett.* **35**, 577 (1975).
- [2] For recent results, see *Non-neutral Plasma Physics II*, edited by J. Fajans and D.H.E. Dubin, AIP Conf. Proc. No. 331 (AIP, New York, 1995).
- [3] J.N. Tan, J.J. Bollinger, and D.J. Wineland, *IEEE Trans. Instrum. Meas.* **44**, 144 (1995).
- [4] S.L. Gilbert, J.J. Bollinger, and D.J. Wineland, *Phys. Rev. Lett.* **60**, 2022 (1988); J.N. Tan *et al.*, *Phys. Rev. Lett.* **75**, 4198 (1995).
- [5] G. Gabrielse *et al.*, *Phys. Rev. Lett.* **65**, 1317 (1990).
- [6] T.J. Murphy and C.M. Surko, *Phys. Rev. A* **46**, 5696 (1992).
- [7] For a review, see T.M. O'Neil, in *Non-neutral Plasma Physics*, edited by Gerry M. Bunce, AIP Conf. Proc. No. 175 (AIP, New York, 1988), p. 1.
- [8] Torques from *rotating* neutral gas are considered in A.J. Peurrung and S.E. Barlow, *Phys. Plasmas* **3**, 2859 (1996).
- [9] J.H. Malmberg and C.F. Driscoll, *Phys. Rev. Lett.* **44**, 654 (1980); C.F. Driscoll, K.S. Fine, and J.H. Malmberg, *Phys. Fluids* **29**, 2015 (1986).
- [10] D.L. Eggleston, T.M. O'Neil, and J.H. Malmberg, *Phys. Rev. Lett.* **53**, 982 (1984).
- [11] J. Notte and J. Fajans, *Phys. Plasmas* **1**, 1123 (1994).
- [12] D.J. Heinzen *et al.*, *Phys. Rev. Lett.* **66**, 2080 (1991).
- [13] For a review, see L.S. Brown and G. Gabrielse, *Rev. Mod. Phys.* **58**, 233 (1986).
- [14] C.S. Weimer *et al.*, *Phys. Rev. A* **49**, 3842 (1994).
- [15] Some preliminary results are in F. Anderegg *et al.*, in *Non-neutral Plasma Physics II* (Ref. [2]), p. 1.
- [16] R.E. Pollock and F. Anderegg, in *Non-neutral Plasma Physics II* (Ref. [2]), p. 139.
- [17] S.M. Crooks and T.M. O'Neil, *Phys. Plasmas* **2**, 355 (1995); S.M. Crooks, Ph.D. thesis, Univ. of Calif. at San Diego, 1995 (unpublished).
- [18] R. Fitzpatrick and T.C. Hender, *Phys. Fluids B* **3**, 644 (1991); T.H. Jensen and A.W. Leonard, *ibid.* **3**, 3422 (1991).
- [19] R.A. MacGill, I.G. Brown, and J.E. Galvin, *Rev. Sci. Instrum.* **61**, 580 (1990).
- [20] E. Sarid, F. Anderegg, and C.F. Driscoll, *Phys. Plasmas* **2**, 2895 (1995).
- [21] T.M. O'Neil, *Phys. Fluids* **24**, 1447 (1981).
- [22] B.P. Clugish and C.F. Driscoll, *Phys. Rev. Lett.* **74**, 4213 (1995).
- [23] S.A. Prasad and T.M. O'Neil, *Phys. Fluids* **26**, 665 (1983); J.K. Jennings, R.L. Spencer, and K.C. Hansen, *Phys. Plasmas* **2**, 2630 (1995).